

Imaging the water snowline in protostellar envelopes

Merel L.R. van 't Hoff¹

¹Leiden Observatory, Leiden University, PO box 9513, NL-2300 RA, Leiden, the Netherlands
email: vthoff@strw.leidenuniv.nl

Abstract. Determining the locations of the major snowlines in protostellar environments is crucial to fully understand the planet formation process and its outcome. Despite being located far enough from the central star to be spatially resolved with ALMA, the CO snowline remains difficult to detect directly in protoplanetary disks. Instead, its location can be derived from N_2H^+ emission, when chemical effects like photodissociation of CO and N_2 are taken into account. The water snowline is even harder to observe than that for CO, because in disks it is located only a few AU from the protostar, and from the ground only the less abundant isotopologue H_2^{18}O can be observed. Therefore, using an indirect chemical tracer, as done for CO, may be the best way to locate the water snowline. A good candidate tracer is HCO^+ , which is expected to be particularly abundant when its main destructor, H_2O , is frozen out. Comparison of H_2^{18}O and H^{13}CO^+ emission toward the envelope of the Class 0 protostar IRAS2A shows that the emission from both molecules is spatially anticorrelated, providing a proof of concept that H^{13}CO^+ can indeed be used to trace the water snowline in systems where it cannot be imaged directly.

Keywords. stars: individual (TW Hydrae, NGC1333 IRAS2A), stars: formation, planetary systems: protoplanetary disks, astrochemistry

1. Introduction

The formation of low-mass stars begins with the collapse of a dense core in a molecular cloud. To conserve angular momentum, the infalling material forms a disk around the protostar. Due to the ongoing accretion of material from the surrounding envelope through the disk onto the star, together with the launching of an outflow, the envelope dissipates over time. What remains is a pre-main sequence star surrounded by a protoplanetary disk that contains the gas and dust from which a planetary system may be forming. The composition of the planets is thus determined by the chemical structure of the protostellar environment.

A key aspect of protostellar chemistry are snowlines. A snowline marks the midplane radius at which a molecular species freezes out from the gas phase onto dust grains. The location of a snowline depends both on the species-dependent sublimation temperature and the physical structure of the protostellar envelope or protoplanetary disk (e.g., temperature and density; see Fig. 1). The selective freeze out of major carbon or oxygen carrying species at different snowlines causes the elemental C/O-ratio of the planet forming material to vary with radial distance from the star (Öberg et al. 2011; Öberg & Bergin 2016). The bulk composition of planets may therefore be regulated by their formation location with respect to the major snowlines (e.g., Madhusudhan et al. 2014; Walsh et al. 2015; Eistrup et al. 2016). Moreover, the growth of dust particles, and thus the planet formation efficiency is thought to be enhanced in these freeze-out zones, for example due to the increase in solid density (e.g., Stevenson & Lunine 1988; Ros & Johansen 2013; Schoonenberg & Ormel 2017). Snowlines thus play a crucial role in the formation and

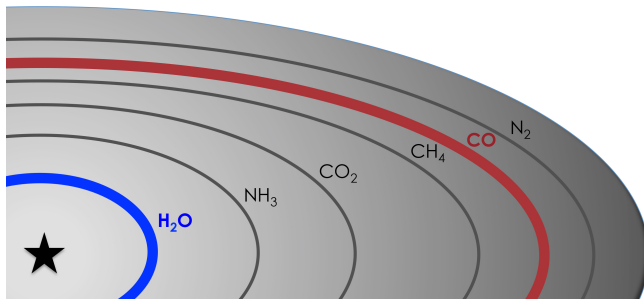


Figure 1. Schematic overview of the major snowlines. Their relative positions are set by the species-dependent freeze-out temperature, while the absolute positions depend on the physical structure of each individual object. The CO and H₂O snowlines discussed here are highlighted.

composition of planets. Determining their locations is therefore key to fully understand the planet formation process and its outcome.

2. The CO snowline

Of the major snowlines, the CO snowline is particularly interesting because CO ice is the starting point for the formation of many complex organic molecules (e.g., Herbst & van Dishoeck 2009). In addition, due to the low sublimation temperature of CO (~ 20 K), the CO snowline is located relatively far away from the central star (10s–100 AU in protoplanetary disks; see Fig. 1). Although we are now able to spatially resolve this with ALMA, locating the CO snowline directly remains difficult. CO line emission is generally optically thick and does not reveal the cold disk midplane. The logical step in such situation would be to use optically thin isotopologues. However, even C¹⁸O does not always offer a solution as is seen for TW Hya (Schwarz et al. 2016): the CO abundance remains 1–2 orders of magnitude below the 10^{-4} ISM abundance far within the radius where the CO snowline is expected based on the disk temperature. Furthermore, a recent ALMA survey of all disks in the Lupus star forming region suggest that CO abundances below the ISM abundance may be common (Ansdell et al. 2016; Miotello et al. 2017), indicating that other processes than freeze-out may contribute to lowering the gas-phase CO abundance. In contrast to C¹⁸O, the double isotopologue ¹³C¹⁸O has recently been shown to reveal the snowline location in TW Hya (Zhang et al. 2017). However, the low ¹³C¹⁸O abundance restricts observations to the very few nearest and brightest disks.

An alternative approach is to use a molecule whose abundance is strongly affected by the freeze-out of CO. One such molecule is DCO⁺, which forms via reaction of H₂D⁺ and CO. Based on these chemical considerations, DCO⁺ emission is expected to form a ring inside the CO snowline, where the CO abundance is low enough to enhance H₂D⁺ formation, while there is still enough gaseous CO left to act as parent molecule for DCO⁺. Mathews et al. (2013) indeed observed ring-shaped DCO⁺ emission toward HD 163296, but the outer radius was later shown not to correspond exactly to the CO snowline (Qi et al. 2015); probably because DCO⁺ can also form in warmer regions higher up in the disk from CH₂D⁺ (Favre et al. 2015). ALMA observations of six protoplanetary disks by Huang et al. (2017) corroborate that DCO⁺ emission, while still tracing relatively cold gas, does not have a direct relation with the CO snowline in disks.

Another molecule suggested to trace the CO snowline is N₂H⁺. Formation of N₂H⁺ occurs through proton transfer from H₃⁺ to N₂,



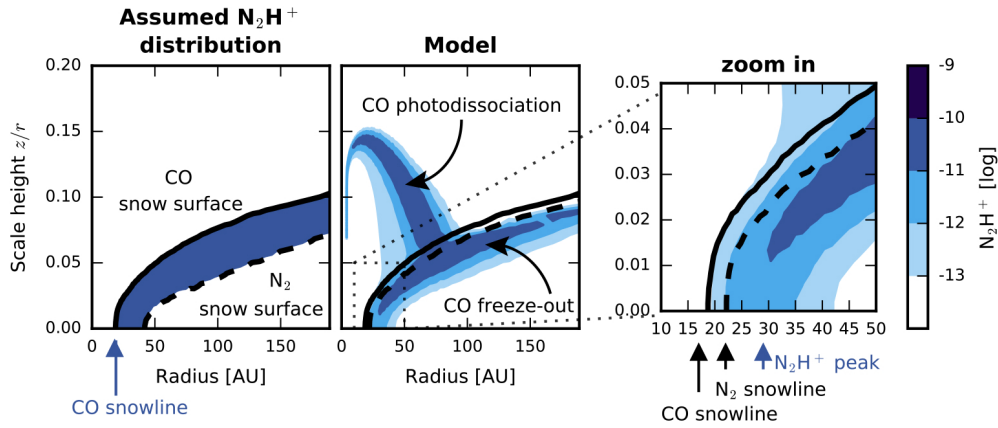
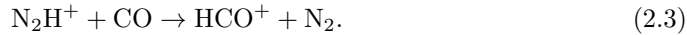


Figure 2. Generally assumed N_2H^+ distribution in protoplanetary disks, i.e., between the CO and N_2 snow surfaces (*left panel*) and the N_2H^+ distribution for TW Hya as predicted by our simple chemical model (*middle panel*). A zoom in on the region around the snowlines is shown in the *right panel*. The solid line indicates the CO snow surface and the dashed line the N_2 snow surface. The crucial differences between the expectations and the model predictions are the location of N_2H^+ peak (at the CO snowline versus beyond the CO and N_2 snowlines, resp.), and the formation of N_2H^+ above the CO snow surface in the model.

but is impeded when CO is present in the gas phase because CO competes with N_2 for reaction with H_3^+ ,



In addition, reaction with gaseous CO is the dominant destruction route of N_2H^+ :



N_2H^+ is therefore expected to be abundant only beyond the CO snowline, where CO is depleted from the gas phase. A CO snowline location has indeed been derived from N_2H^+ emission for the disks around TW Hya and HD 163296 (Qi et al. 2013, 2015).

However, a simple chemical model incorporating the main reactions for N_2H^+ (Eqs. 2.1–2.3) in addition to freeze out, thermal desorption and photodissociation of CO and N_2 , combined with radiative transfer modeling, shows that the relationship between N_2H^+ and the CO snowline is more complicated (van ’t Hoff et al. 2017a). First, the N_2H^+ abundance peaks at temperatures slightly below the CO freeze-out temperature, instead of directly at the CO snowline (see Fig. 2), as also found by Aikawa et al. (2015). The snowline marks the radius where 50% of the CO is present in the gas phase and 50% is frozen out. Apparently, this reduction in gaseous CO is not yet enough to diminish the N_2H^+ destruction. Second, N_2H^+ can be formed higher up in the disk, above the layer where CO is frozen out, due to a small difference in the photodissociation rates for CO and N_2 (see Fig. 2). The slightly higher rate for CO creates another region where N_2 is still present in the gas phase, while CO is not. This “surface” layer of N_2H^+ can contribute significantly to the emission, shifting the N_2H^+ emission peak to larger radii, away from the CO snowline. N_2H^+ emission alone then merely provides an upper limit for the snowline location.

Applying our modeling approach to the TW Hya disk, using the physical model from Kama et al. (2016), we derive a CO snowline location of ~ 18 AU, instead of the ~ 30 AU suggested by Qi et al. (2013). The latter authors fitted a radial N_2H^+ column density profile to the emission with a steep rise at the CO snowline. Our outcome is consistent

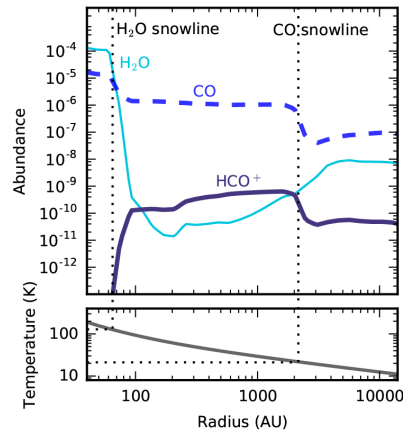


Figure 3. Temperature profile for the NGC1333 IRAS2A envelope from Kristensen et al. (2012) (*bottom panel*), and the corresponding H_2O (thin solid line), CO (dashed line) and HCO^+ (thick solid line) abundances predicted by the three-phase astrochemical model GRAINOBLE (*top panel*). The vertical dotted lines mark the H_2O and CO snowlines around 100 K and 20 K, resp.

with the results from Schwarz et al. (2016) based on multiple ^{13}CO and C^{18}O lines, and the $^{13}\text{C}^{18}\text{O}$ analysis by Zhang et al. (2017). Deriving the CO snowline location from N_2H^+ emission is thus not as straightforward as was generally assumed, but, given a good physical model for the target disk, the location can be determined using simple chemistry in combination with radiative transfer modeling.

3. The H_2O snowline

The most important snowline is the water snowline, since the bulk of the oxygen budget and ice mass is in water ice. Unfortunately, this snowline is even more difficult to observe than that for CO . Because of the large binding energy of H_2O , water sublimates off the grains only at temperatures above ~ 100 K. This means that the snowline is located a few AU from the star in protoplanetary disks, that is, $\sim 0.01''$ in the nearest star-forming region Taurus. High angular resolution is thus required to observe it. Furthermore, except for the H_2O line at 183 GHz, the only thermal water lines observable from the ground are those from the less abundant isotopologue H_2^{18}O . As such, even ALMA will have great difficulty to detect the water snowline in protoplanetary disks. Cold water lines (< 100 K) have been detected from space toward TW Hya with *Herschel* (Hogerheijde et al. 2011), but the *Herschel* beam is too large to resolve the snowline. So far, only for the disk around V883 Ori a snowline location has been reported, but this was inferred from a steep drop in the dust optical depth (Cieza et al. 2016).

The best way to locate the water snowline may therefore be by applying the same strategy as done for CO , that is, using a chemical tracer. The best candidate to trace the water snowline is HCO^+ , because gaseous H_2O is its most abundant destroyer (Phillips et al. 1992; Bergin et al. 1998). A strong decline in HCO^+ abundance is thus expected when H_2O desorbs from the dust grains. This is corroborated by the results from chemical models. Figure 3 shows the outcome of the three-phase astrochemical code GRAINOBLE (Taquet et al. 2014) for the 1D temperature and density structure of the envelope around NGC1333 IRAS2A (Kristensen et al. 2012). Three-phase models consider reactions for gas-phase species, reactions for species on the ice surface, and reactions for bulk ice species. As expected, the HCO^+ and H_2O abundances show a strong anticorrelation.

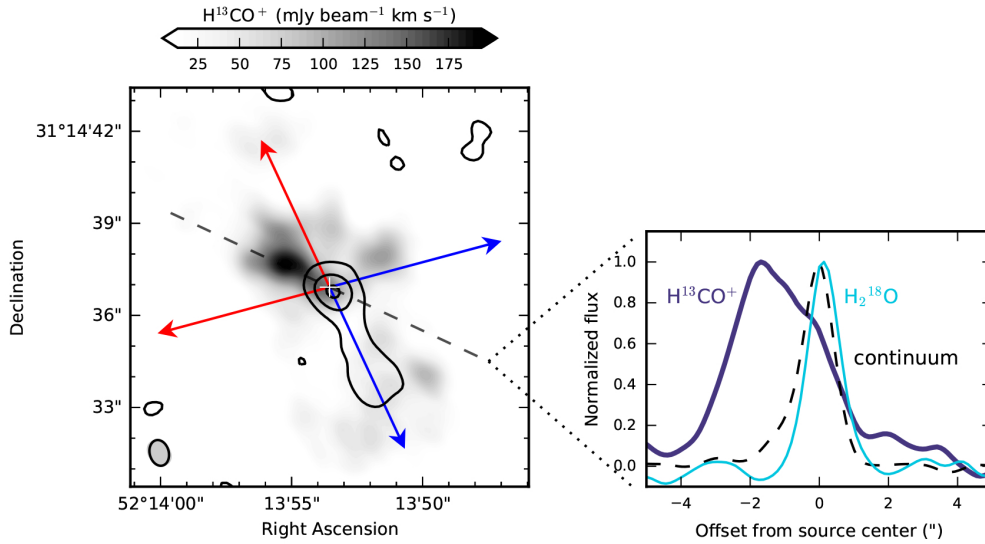


Figure 4. Integrated continuum subtracted intensity map for the H^{13}CO^+ $J = 3 - 2$ transition (grey scale) toward IRAS2A with the H_2^{18}O $3_{1,3} - 2_{2,0}$ transition overlaid in contours (*left panel*). The H_2^{18}O contours are shown at $8.2 (1\sigma) \times [3, 15, 35]$ $\text{mJy beam}^{-1} \text{ km s}^{-1}$. The position of the continuum peak is marked by a white cross and the outflow axes by arrows. Both observations have a similar beam size (depicted in the lower left corner). The *right panel* shows the integrated intensities for H^{13}CO^+ (thick solid line), H_2^{18}O (thin solid line) and the continuum (dashed line) along the dashed line, normalized to their maximum value.

Hints of this anticorrelation are seen in observations towards the protostar IRAS 15398-3359, which show ring-shaped H^{13}CO^+ emission surrounding CH_3OH emission, another grain-surface molecule with a similar snowline location as water (Jørgensen et al. 2013). The non-detection of the high excitation H_2^{18}O $4_{1,4} - 3_{2,1}$ line prevented unambiguous confirmation, but the detected HDO emission, although more complex, is consistent with the $\text{H}_2\text{O}-\text{HCO}^+$ anticorrelation scenario (Bjerkeli et al. 2016).

Protostellar envelopes, like IRAS 15398-3359, are the best sources to establish whether HCO^+ is a good snowline tracer: the water snowline is located further away from the star than in disks (10s–100s AU rather than a few AU; Harsono et al. 2015; Cieza et al. 2016), and compact warm water has already been observed toward four sources (Jørgensen & van Dishoeck 2010; Persson et al. 2012, 2013; Taquet et al. 2013). The only thing lacking are thus HCO^+ observations. We have therefore observed the optically thin isotopologue H^{13}CO^+ toward the Class 0 protostar NGC1333 IRAS2A using NOEMA (van 't Hoff et al. 2017b). Comparison with the H_2^{18}O emission presented by Persson et al. (2012) shows that while H_2^{18}O peaks on source, H^{13}CO^+ has its emission peak $\sim 2''$ off source (see Fig. 4). As a first analysis, we performed a 1D radiative transfer calculation with Ratran (Hogerheijde & van der Tak 2000), using the 1D temperature and density structure derived by Kristensen et al. (2012) from DUSTY modeling (Ivezić & Elitzur 1997) of the continuum emission. A simple parametrized abundance profile for H^{13}CO^+ with sharp decreases inside the H_2O snowline and outside the CO snowline, as predicted by a full chemical model, can reproduce the observed location of the emission peak (see Fig. 5). The H^{13}CO^+ abundance drops outside the CO snowline because its parent molecule, CO, is frozen out. The temperature, however, has to be increased by a factor of ~ 2 to reproduce the observed peak location with a drop in H^{13}CO^+ at 100 K. A constant

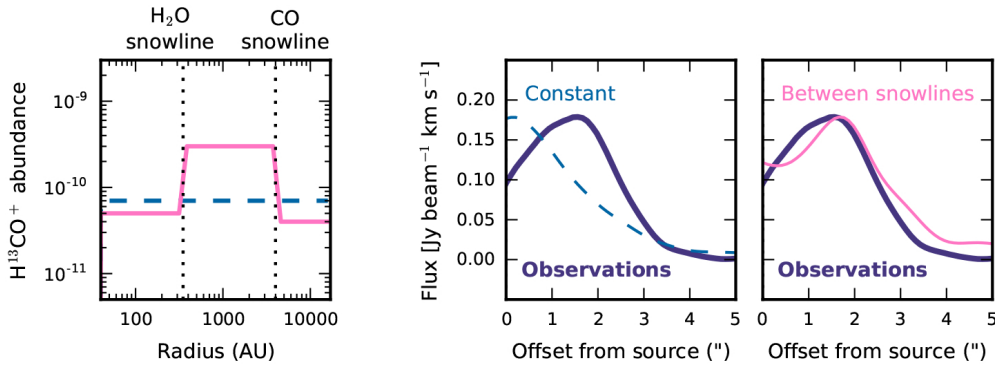


Figure 5. Different H^{13}CO^+ abundance profiles (*left panel*) and the resulting simulated integrated emission along the northeastern part of the radial cut shown in Fig. 4 (*right panels*). The vertical dotted lines in the *left panel* mark the H_2O and CO snowlines around 100 K and 20 K, resp. The observed H^{13}CO^+ emission is shown with the thick solid lines in the *right panels*.

H^{13}CO^+ abundance at all radii, on the other hand, produces emission peaking on source, unlike observed. These results suggest that water and HCO^+ are indeed anticorrelated, and provide a proof of concept that the optically thin isotopologue H^{13}CO^+ can be used to trace the water snowline.

4. Summary and outlook

Due to its close proximity to the central star and the fact that only the less abundant isotopologue H_2^{18}O can be observed from the ground, both high angular resolution and high sensitivity are required to observe the water snowline. Chemical imaging may therefore be the only way to locate this snowline in protoplanetary disks. This approach has proven useful for the CO snowline, although simple chemical considerations have to be taken into account when deriving the CO freeze-out radius from N_2H^+ emission. The best candidate to image the water snowline is HCO^+ , because its main destructor is gaseous H_2O . The first observations of both H^{13}CO^+ and H_2^{18}O toward the protostellar envelope of NGC1333 IRAS2A show that these molecules are indeed spatially anti-correlated. This suggest that H^{13}CO^+ may be used as a tracer of the water snowline in protoplanetary disks.

Acknowledgments

I would like to acknowledge and thank Catherine Walsh, Mihkel Kama, Stefano Facchini, Magnus Persson, Daniel Harsono, Vianney Taquet, Jes Jørgensen, Ruud Visser, Edwin Bergin and Ewine van Dishoeck for their contributions to this work, and support from a Huygens fellowship from Leiden University.

References

- Aikawa, Y., Fura, K., Nomura, H., & Qi, C. 2015, *ApJ*, 807, 120
 Ansdell, M., Williams, J.P., van der Marel, N. 2016, *ApJ*, 828, 46
 Bergin, E.A., Melnick, G.J., & Neufeld, D.A. 1998, *ApJ*, 499, 777
 Bjerkele, P., Jørgensen, J.K., Bergin, E.A., *et al.* 2016, *A&A*, 595, A39
 Cieza, L.A., Casassus, S., Tobin, J., *et al.* 2016, *Nature*, 535, 258

- Eistrup, C., Walsh, C., & van Dishoeck, E.F. 2016, *A&A*, 595, A83
- Favre, C., Bergin, E.A., Cleeves, L.I., Hersant, F., Qi, C., & Aikawa, Y. 2015, *ApJL*, 802, L23
- Herbst, E., & van Dishoeck, E.F. 2009, *ARA&A*, 47, 427
- Harsono, D., Bruderer, S., & van Dishoeck, E.F. 2015, *A&A*, 582, A41
- Hogerheijde, M.R., & van der Tak, F.F.S. 2000, *A&A*, 362, 697
- Hogerheijde, M.R., Bergin, E.A., Brinch, E.A., *et al.* 2011, *Science*, 334, 338
- Huang, J., Öberg, K.I., Qi, C., *et al.* 2017, *ApJ*, 835, 231
- Ivezić, Z., & Elitzur, M. 1997, *MNRAS*, 287, 799
- Jørgensen, J.K., & van Dishoeck, E.F. 2010, *ApJL*, 710, L72
- Jørgensen, J.K., Visser, R., Sakai, N., *et al.* 2013, *ApJL*, 779, L22
- Kama, M., Bruderer, S., van Dishoeck, E.F., *et al.* 2016, *A&A*, 592, A83
- Kristensen, L.E., van Dishoeck, E.F., Bergin, E.A., *et al.* 2012, *A&A*, 542, A8
- Madhusudhan, N., Amin, M.A., & Kennedy, G.M. 2014, *ApJL*, 794, L12
- Mathews, G.S., Klaassen, P.D., Juhász, A., *et al.* 2013, *A&A*, 557, A132
- Miotello, A., van Dishoeck, E.F., Williams, J.P., *et al.* 2017, *A&A*, 599, A113
- Öberg, K.I., Murray-Clay, R., & Bergin, E.A. 2011, *ApJL*, 743, L16
- Öberg, K.I., & Bergin, E.A. 2016, *ApJL*, 831, L19
- Persson, M.V., Jørgensen, J.K., & van Dishoeck, E.F. 2012, *A&A*, 541, A39
- Persson, M.V., Jørgensen, J.K., & van Dishoeck, E.F. 2013, *A&A*, 549, L3
- Phillips, T.G., van Dishoeck, E.F., & Keene, J. 1992, *ApJ*, 399, 533
- Qi, C., Öberg, K.I., Wilner, D.J., *et al.* 2013, *Science*, 341, 630
- Qi, C., Öberg, K.I., Andrews, S.M., *et al.* 2015, *ApJ*, 813, 128
- Ros, K., & Johansen, A. 2013, *A&A*, 552, A137
- Schoonenberg, D., & Ormel, C.W. 2017, *A&A*, 602, A21
- Schwarz, K., Bergin, E.A., Cleeves, L.I., *et al.* 2016, *ApJ*, 823, 91
- Stevenson, D.J., & Lunine, J.I. 1988, *Icarus*, 75, 146
- Taquet, V., López-Sepulcre, A., Ceccarelli, C., *et al.* 2013, *ApJL*, 768, L29
- Taquet, V., Charnley, S.B., & Sipilä, O. 2014, *ApJ*, 791, 1
- van 't Hoff, M.L.R., Walsh, C., Kama, M., Facchini, S., & van Dishoeck, E.F. 2017a, *A&A*, 599, A101
- van 't Hoff, M.L.R., Persson, M.V., Harsono, D., *et al.* 2017b, *A&A*, submitted
- Walsh, C., Nomura, H., & van Dishoeck, E.F. 2015, *A&A*, 582, A88
- Zhang, K., Bergin, E.A., Blake, G.A., Cleeves, L.I., & Schwarz K.R. 2017 *Nat. Astron.*, 1, 0130